Pergamon

Energy 27 (2002) 715–727

ENERGY

www.elsevier.com/locate/energy

Collector efficiency of double-flow solar air heaters with fins attached

H.-M. Yeh *, C.-D. Ho, J.-Z. Hou

Department of Chemical Engineering, Tamkang University, Tamsui, Taipei 251, Taiwan, ROC

Abstract

A design for inserting an absorbing plate to divide the air duct into two channels (the upper and the lower) for double-flow operation in solar air heaters with fins attached over and under the absorbing plate has been investigated both experimentally and analytically. The present work is restricted to the case where the outside air is being heated directly, and the configuration investigated here will have lower collector efficiency if the inlet-air temperature is substantially higher than the ambient temperature because of the far greater potential for heat loss from the top. However, the double-flow device introduced here was designed for creating a solar collector with heat-transfer area double between the absorbing plate and heated air. This advantage may compensate for the heat loss from the top when the inlet-air temperature is higher than the ambient temperature. The agreement of the theoretical predictions with those measured values from the experimental results is fairly good. Considerable improvement in collector efficiency of solar air heaters with fins attached is obtained by employing such a double-flow device, instead of using a single-flow example and operating at the same total flow rate. Both the theoretical predictions and experimental results showed that the optimal fraction of airflow rate in upper and lower subchannels is around the value of 0.5. The effect of the flow-rate ratio of the two air streams of flowing over and under the absorbing plate on the enhancement of collector efficiency is also investigated.

1. Introduction

A flat plate solar air heater, in its simplest form, consists of one or more sheets of glass or transparent material situated above an absorbing plate with the air flowing either over or under the absorbing plate [1–7]. One way to achieve considerable improvement in collector efficiency is to use an extended heat-transfer area [8] by attaching fins to a flat-plate type of solar air heater. Recently, several investigators designed two-pass operations with internal or external reflux at

* Corresponding author. Tel.: +886-2-2625656x2601; fax: +886-2-26209887.
E-mail address: hmyeh@che.tku.edu.tw (H..-M. Yeh).

0360-5442/02/$ - see front matter
PII: S0360-5442(02)00010-5

Nomenclature

A_c Surface area of the collector, LB (m^2)
A_f Total surface area of fins, (m^2)
C_p Specific heat of air at constant pressure (kJ kg^{-1} K^{-1})
H Height of the air tunnels in a double-flow solar collector, or half height of the air tunnel in a single-flow solar collector (m)
h_1,h_2,h'_1,h'_2 convective heat-transfer coefficient for fluid flowing over a flat plate (kJ h^{-1} m^{-2} K^{-1})
h_r Radiant heat-transfer coefficient between two parallel plates (kJ h^{-1} m^{-2} K^{-1})
I Improvement of collector performance
k Thermal conductivity of fin (kJ h^{-1} m^{-1} K^{-1})
L Collector length (m)
m Mass-flow rate of air (kg h^{-1})
n Number of fins on an absorbing plate, B/w_1
N The number of experimental measurements
Q_u Useful gain of energy carried away by air per unit time (kJ h^{-1})
Q_{u1},Q_{u2} Useful gains of energy brought out by fluid 1 and fluid 2 in the upper- and lower-flow channels, respectively (kJ h^{-1})
r The fraction of mass-flow rate, rm and $(1-r)m$ in upper and lower channels, respectively
S_0 Incident solar radiation (W m^{-2})
$S_{\eta i}$ The precision index of an individual measurement
$S_{\bar{\eta} i}$ The mean value of $S_{\eta i}$
T_a Ambient temperature (K)
T_{fi} Fluid temperatures (K), $i = 1,2$
$T_{i,0}$ Outlet temperatures of fluids (K), $i = 1,2$
T_{in} Inlet temperature of fluid (K)
t Thickness of the fins (m)
U_B Loss coefficient from the surfaces of edges and the bottom of the solar collector to the ambient (kJ h^{-1} m^{-2} K^{-1})
U_L Overall loss coefficient (kJ h^{-1} m^{-2} K^{-1})
U_T Loss coefficient from the absorbing plate through the top of solar collector to the ambient (kJ h^{-1} m^{-2} K^{-1})
w_1 Distance between fins (m)
w_2 Height of the fins (m)
α_p Absorptivity of the absorbing plate
η,η_D Collector efficiency of double-flow type and downward-type single-flow solar air heaters
$\eta_{f,i}$ Fin efficiency, $i = 1,2$
η_i Experimental data of η
$\hat{\eta}_i$ Theoretical prediction η
ϕ_i Dimensionless quantity defined by Eq. (5)

τ_g Transmittance of the glass cover
ε_g, ε_p, ε_R Emissivity of the glass cover, absorbing plate, bottom plate
ρ Air density (kg m^{-3})
μ Air viscosity (kg m^{-1} h^{-1})
σ Stefan–Boltzmann constant (kJ h^{-1} m^{-2} K^{-4}), 2.04×10^{-7}

the other end. Satcunanathan and Deonarine [9] constructed a two-pass air heater in which the air flows through the glass panes before passing through the blackened metal collector. Wijeysundera et al. [10] developed two-pass flow arrangements, and the design curves for those devices over a range of variables were also presented. Garg et al. [11] developed the theory of multiple-pass solar air heaters. It is well known that the collector configuration will influence the fluid velocity as well as the strength of forced convection. A simple procedure for changing the fluid velocity as well as the strength of forced convection involved adjusting the aspect ratio of a rectangular flat-plate collector with constant flow rate [12].

The collector efficiency of double-flow solar air heaters with fins attached has been investigated both experimentally and theoretically here. The present work is restricted to the case where the outside air is being heated directly, and the configuration investigated here will have lower collector efficiency if the inlet-air temperature is substantially higher than the ambient temperature because of the far greater potential for heat loss from the top. The unglazed transpired plate (UTP) collector recently developed and extensively studied by many investigators [13–17], is not only simple and inexpensive in design but can also avoid losing substantial heat from the top. However, the double-flow device introduced here was designed for creating a solar collector with heat-transfer area double (upper and lower absorbing surfaces). This advantage may compensate for the heat loss from the top when the inlet-air temperature is higher than the ambient temperature.

2. Theory

Fig. 1 shows a solar air heater with fins attached in which the absorbing plate divides the air conduit into two parts, channel 1 and channel 2, while the energy-flow diagram of such a device is presented in Fig. 2. As seen in Fig. 2, two air streams (fluid 1 and fluid 2), of different flow rates but with total flow rate fixed, flow steadily and simultaneously through two such separated channels (over and under the absorbing plate) of the same size for heating. The following assumptions are made in the present analysis: the temperatures of the absorbing plate, bottom plate and bulk fluids are functions of the flow direction only, and both the glass covers and fluids do not absorb radiant energy.

2.1. Fin efficiency

The rates of convective heat transfer from the absorbing surfaces to the flowing air in channels 1 and 2, respectively, are:

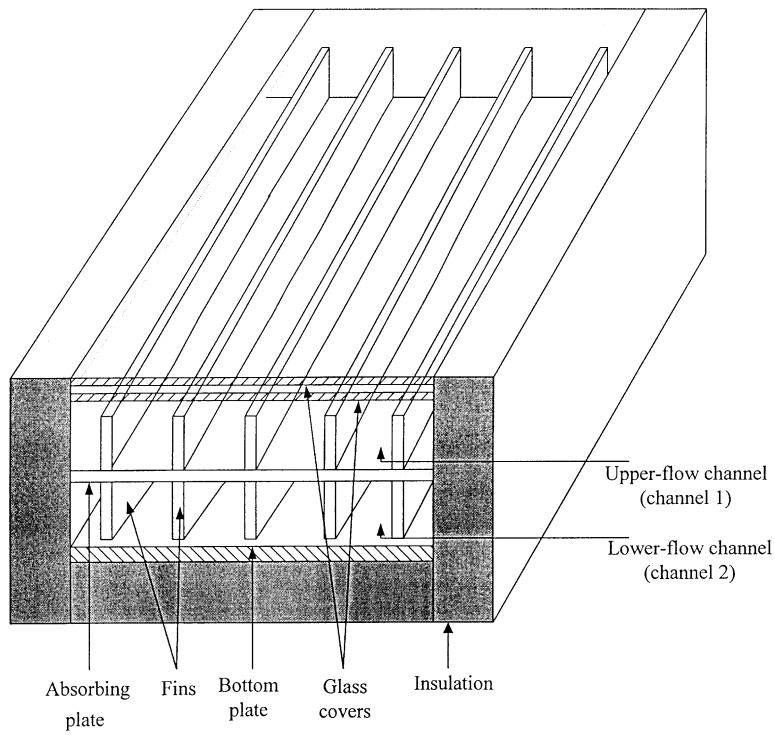

Fig. 1. Double-flow solar air heater with fins attached.

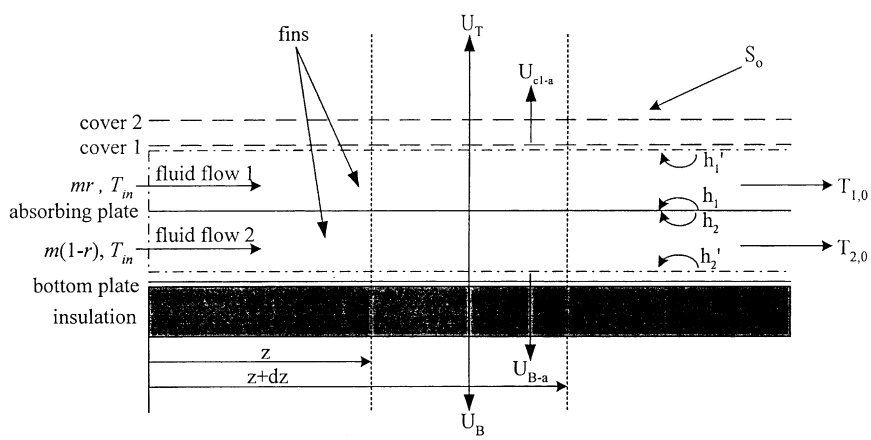

Fig. 2. Energy-flow diagram of double-flow solar air heater with fins attached.

$$q_1 = h_1 A_c (T_p - T_{f_1}) \tag{1}$$

and

$$q_2 = h_2 A_c (T_p - T_{f_2}). \tag{2}$$

If the absorbing surfaces are attached by fins, then [8]

$$q_1 = h_1\phi_1 A_c(T_p - T_{f_1}) \tag{3}$$

and

$$q_2 = h_2\phi_2 A_c(T_p - T_{f_2}), \tag{4}$$

where

$$\phi_i = 1 + (A_{f,i}/A_c)\eta_{f,i} \tag{5}$$

and

$$\eta_{f,i} = \frac{\tanh\sqrt{2h_i w_2/kt}}{2h_i w_2/kt} \tag{6}$$

Note that $\phi_i = 1$ when there is no fin attached on the absorbing plate.

2.2. Useful gain of energy

The method for theoretical prediction of collector efficiencies as well as the experimental procedure is similar to that presented in our previous work [18], except that allowance is made for the fins to be attached to the upper and lower surfaces of the absorbing plate. The useful energy gains brought out by fluid 1 and fluid 2 in the upper- and lower-flow channels, respectively, are

$$Q_{u1} = mrC_p(T_{1,0} - T_{in}) = MrA_c(T_{1,0} - T_{in}), \tag{7}$$

and

$$Q_{u2} = m(1-r)C_p(T_{2,0} - T_{in}) = M(1-r)A_c(T_{2,0} - T_{in}). \tag{8}$$

In Eqs. (7) and (8)

$$M = mC_p/nw_1L = mC_p/A_c \tag{9}$$

and the outlet temperatures of fluid, $T_{1,0}$ and $T_{2,0}$ may be calculated from Eqs. (10) and (11), respectively [18]

$$T_{1,0} = \frac{Y_1 - B_5/(1-r)}{B_4/(1-r)}C_1 e^{(Y_1/M)} + \frac{Y_2 - B_5/(1-r)}{B_4/(1-r)}C_2 e^{(Y_2/M)} - \frac{B_5(B_3B_4 - B_1B_6)}{B_4(B_1B_5 - B_2B_4)} - \frac{B_6}{B_4} + T_a \tag{10}$$

and

$$T_{2,0} = C_1 e^{(Y_1/M)} + C_2 e^{(Y_2/M)} - \frac{B_3B_4 - B_1B_6}{B_1B_5 - B_2B_4} + T_a, \tag{11}$$

where

$$Y_1 = \left[\left(\frac{B_1}{r} + \frac{B_5}{1-r}\right) + \sqrt{\left(\frac{B_1}{r} - \frac{B_5}{1-r}\right)^2 + \frac{4B_2B_4}{r(1-r)}}\right] \Big/ 2, \tag{12}$$

and

$$Y_2 = \left[\left(\frac{B_1}{r} + \frac{B_5}{1-r}\right) + \sqrt{\left(\frac{B_1}{r} - \frac{B_5}{1-r}\right)^2 + \frac{4B_2B_4}{r(1-r)}}\right] \Big/ 2, \tag{13}$$

$$C_1 = -\left(\frac{B_4/(1-r) + B_5/(1-r) - Y_2}{Y_2 - Y_1}(T_{in} - T_a) + \frac{Y_2(B_3B_4 - B_1B_6)}{(Y_2 - Y_1)(B_1B_5 - B_2B_4)} + \frac{B_6/(1-r)}{Y_2 - Y_1}\right) \tag{14}$$

and

$$C_2 = \frac{B_4/(1-r) + B_5/(1-r) - Y_1}{Y_2 - Y_1}(T_{in} - T_a) - \frac{Y_1(B_3B_4 - B_1B_6)}{(Y_2 - Y_1)(B_1B_5 - B_2B_4)} + \frac{B_6/(1-r)}{Y_2 - Y_1} \tag{15}$$

while all the coefficients, B's, are in terms of the convective heat-transfer coefficient, loss coefficients, physical properties and dimensionless quantities ϕ_i, as referred to in Appendix A.

2.3. Collector efficiency

The total energy gain is

$$Q_u = Q_{u_1} + Q_{u_2}, \tag{16}$$

thus, the collector efficiency is obtained from Eqs. (7), (8) and (16) as

$$\eta = \frac{Q_u/A_c}{S_0} = (M/S_0)[rT_{1,0} + (1-r)T_{2,0} - T_{in}]. \tag{17}$$

3. Experimental studies

3.1. Apparatus and procedure

A double-flow solar air heater was built for the experiment, which is exactly the same as that employed in the previous work [18] except that fins were attached to both upper and lower surfaces of the absorbing plate, as shown in Fig. 1, to extend the heat-transfer area. The fins placed on the black absorbing surfaces have a height of 5.5 cm and a distance of 6 cm between fin center lines. For steady-state operation, the experiment was carried out under artificial simulation using an indoor solar simulator [18], as shown in Fig. 3.

The wind velocity was set at 1 m/s, and temperatures of the ambient and inlet air were controlled at 30 °C by using an air conditioner. At the end of each experimental run, air temperatures in the interior and at the inlet and the outlet of the collector, as well as the mass-flow rate of air, were measured. The experimental values of the collector efficiency were then calculated from Eq. (17) and the results given in Table 1 are also plotted in Fig. 4.

3.2. Comparison of theoretical predictions with experimental results

The method for theoretical predictions of collector efficiencies from Eqs. (3)–(17), as well as the use of the empirical equations for calculating the heat-transfer coefficients, have been described in

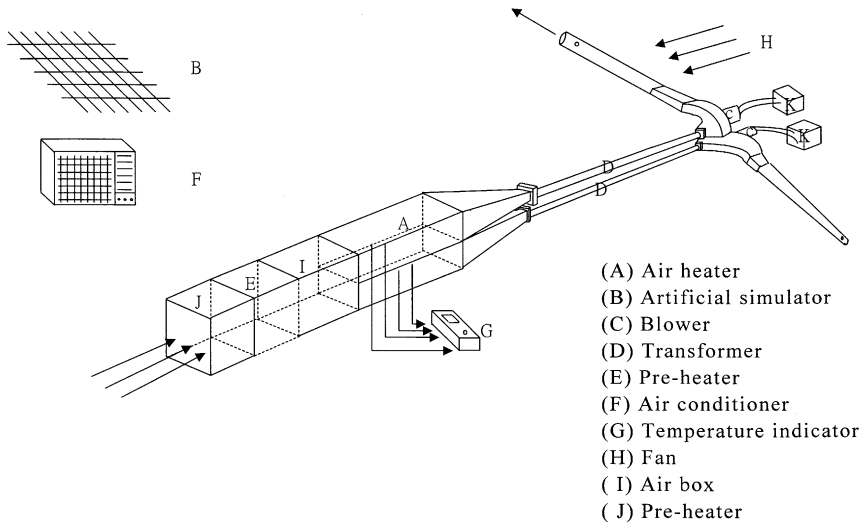

Fig. 3. Experimental apparatus.

the previous work [18]. The physical properties of air are given in Table 2 [19] and the experimental conditions employed in this work are as follows: $L = 30$ cm; $H = 2.75$ cm; $W = 30$ cm; $t = 0.1$ cm; $\tau_g = 0.875$; $\alpha_P = 0.96$; $\varepsilon_g = 0.94$; $\varepsilon_p = 0.8$; $\varepsilon_R = 0.94$; $U_B = h_S/l_s \approx 0$; $T_a = 30°C$; $V = 1.0$m/s; $T_{in} = (30 \pm 0.1)°C$; $S_0 = 830$ and 1100 W m^{-2}; $m = 38.52$; 57.96 and 77.04 kg h^{-1}; $r = 0.2$, 0.4, 0.5, 0.6 and 0.8; $w_1 = 6$cm, $w_2 = 5.5$cm. By substituting the specified values into the appropriate equations, the theoretical predictions were obtained and are also represented in Fig. 4 for comparison. It is seen that the experimental results fairly confirm the theoretical predictions.

4. Results and discussion

4.1. Convection in the upper channel

In addition to the forced convection in the upper-flow channel, actually, there also exists natural convection which, in general, should be taken into consideration. However, within the experimental range of present study, the flows are turbulent and thus, forced convection was dominated. Accordingly, for theoretical confirmation with the experimental results, only forced convection was considered. It is justified in Fig. 4 that the treatment of this convection in the upper-flow channel is acceptable.

4.2. Experimental error

As referred to Moffat [20], the precision index of an individual measurements, η_i, is determined directly from the data set, as follows:

Table 1
Experimental results

M (kg h^{-1})	S_0 = 830(Wm^{-2})							S_0 = 1100 (Wm^{-2})						
	η_D	η					I* (r = 0.5) (%)	η_D	η					I^* (r = 0.5) (%)
		r = 0.2	r = 0.4	r = 0.5	r = 0.6	r = 0.8			r = 0.2	r = 0.4	r = 0.5	r = 0.6	r = 0.8	
38.52	0.401	0.634	0.648	0.651	0.643	0.631	62.34	0.405	0.640	0.651	0.653	0.645	0.632	61.23
57.96	0.461	0.675	0.686	0.689	0.685	0.674	49.46	0.464	0.680	0.688	0.691	0.687	0.675	48.92
77.04	0.499	0.702	0.703	0.705	0.702	0.691	41.28	0.501	0.696	0.705	0.708	0.706	0.693	41.32

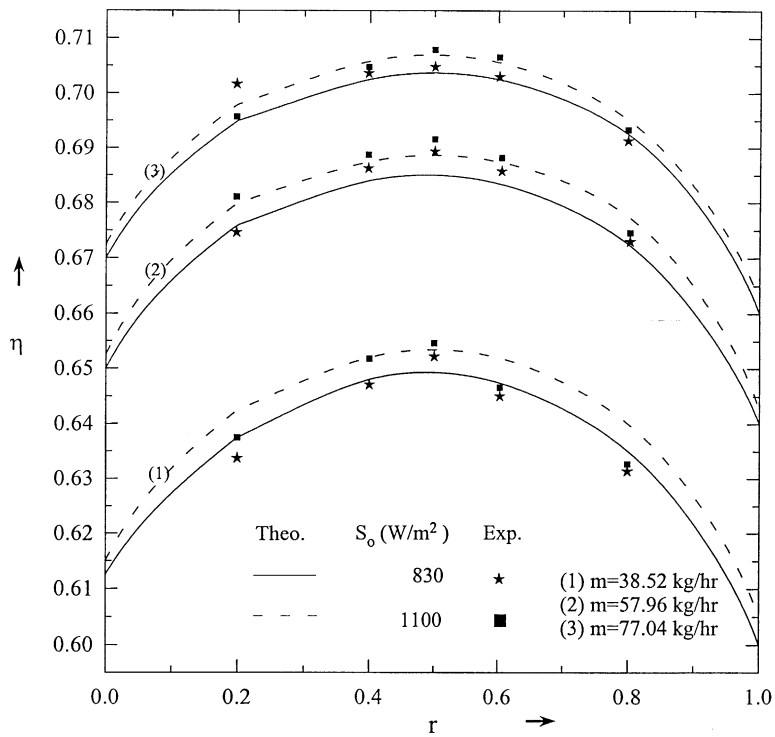

Fig. 4. The theoretical predictions and experimental results of collector efficiencies with the fraction of airflow rate as parameter.

Table 2
Physical properties of air at 1 atm [19]

T (K)	ρ (kg m^{-3})	C_p (kJ kg^{-1} K^{-1})	$\mu \times 10^{-5}$ (kg m^{-1} S^{-1})
250	1.3947	1.006	1.596
300	1.1614	1.007	1.846
350	0.9950	1.009	2.082
400	0.8711	1.014	2.301

$$S_{\eta_i} = \left\{ \sum_i^N \frac{(\eta_i - \bar{\eta}_i)^2}{N-1} \right\}^{1/2} \tag{18}$$

and the resulting uncertainty will be associated with the mean value:

$$S_{\bar{\eta}_i} = \frac{S_{\eta_i}}{\sqrt{N}} \tag{19}$$

The precision index was determined for $S_0 = 830 \mathrm{Wm}^{-2}$ and $S_0 = 1100\ \mathrm{Wm}^{-2}$ with three mass-

flow rates of air. The mean precision index of the experimental measurements in Fig. 4 is $1.29 \times 10^{-4} \leq S_{\bar{\eta}_i} \leq 1.94 \times 10^{-3}$.

The accuracy of the experimental results may be calculated using the definition

$$E = \frac{1}{N} \sum_{i=1}^{N} \frac{|\hat{\eta}_i - \eta_i|}{\hat{\eta}_i}$$

where $\hat{\eta}_i$ denotes the theoretical prediction of η, while η_i, and N are the experimental data of η and the number of experimental measurements, respectively. The error analysis of the five measurements for each experimental run in Fig. 4 is presented in Table 3. It is seen in this table that the agreement between experiment data and the results calculated from the theoretical prediction of the present device is fairly good. Considerable improvement in collector efficiencies was obtained by employing a double-flow solar air heater with fins attached, instead of using a single-flow device of same size and operating at the same total flow rate.

4.3. The effect of r on η

The effect of the fraction of mass transfer rate in upper—(r, fluid 1) or lower—($1-r$, fluid 2) flow channel on the collector efficiency of double-flow solar air heaters with fins attached has been investigated both theoretically and experimentally. As seen in Fig. 4, both the theoretical and experimental results show that the optimal fraction of mass airflow rate ratio, r, for maximum collector efficiency is exactly equal to 0.5 for all operating conditions. It means that in order to achieve the best thermal performance in a double-flow solar air heater with fins attached, in which the cross-section areas of upper-and lower-flow channels are constructed equally, the mass airflow rates in both flow channels must be kept the same. A qualitative agreement is achieved between the theoretical solutions and experimental data. The thermal performance increases with the total mass-flow rate but decreases as r goes away from 0.5.

4.4. The improvement in collector efficiency

The improvement of performance in double-flow solar air heaters is best illustrated by calculating the percentage increase in collector efficiency, based on the downward-type single-flow device with a fixed mass airflow rate m and the same collector size of total height $2H$, i.e.

Table 3
The accuracy of the experimental results

m (kg h^{-1})	$E = \frac{1}{N}\sum_{i=1}^{N}\frac{\lvert\hat{\eta}_i-\eta_i\rvert}{\hat{\eta}_i}$	
	$S_0 = 830(\mathrm{Wm}^{-2})$	$S_0 = 1100(\mathrm{Wm}^{-2})$
38.52	2.61×10^{-3}	4.57×10^{-3}
57.96	4.26×10^{-3}	1.35×10^{-3}
77.04	2.26×10^{-3}	1.07×10^{-3}

$$I^* = \frac{\eta^* - \eta_D}{\eta_D} \tag{20}$$

in which η_D denotes the collector efficiency in a downward-type single-flow solar air heater with fins attached while η^* and I^* are, respectively, the maximum collector efficiency with $r = 0.5$ and the corresponding improvement of collector efficiency, in a double-flow solar air heater with fins attached. For downward-type single-flow solar air heaters with fins attached, the calculation procedure for collector efficiency [8] is much simpler than for double-flow devices, and will not be described here. The experimental results for I^* are shown in Table 1. It is found from Table 1 that the improvements in the collector efficiency decrease with increasing total mass-flow rate and with decreasing incident solar radiation. Considerable improvement of performance is achievable if a double-flow device is employed, instead of using a single-flow one.

5. Conclusion

The equations for theoretical prediction of collector efficiency in double-flow solar air heaters with fins attached on both surfaces of the absorbing plate, have been derived from energy balances with the ratio of airflow rate as the parameter. The double-flow type solar air heaters introduced in present study have the heater-transfer area double, leading to improved thermal performance. The effect of the fraction of mass transfer rate in upper—(r, fluid 1) or lower—($1-r$, fluid 2) flow channel on the collector efficiency of double-flow type solar air heaters with fins attached has been investigated both theoretically and experimentally. Experiment was carried out under the artificial simulation for steady operations. The theoretical predictions are fairly confirmed with the experimental results, as shown in Fig. 4. The accuracy of the experimental results was calculated as shown in Table 3 and the error analysis of the experimental measurements is $1.07 \times 10^{-3} \leq E \leq 4.57 \times 10^{-3}$. Both the theoretical predictions and experimental results show that the optimal ratio of airflow rates in both flow channels for maximum collector efficiency is unity (i.e. the optimal fraction of airflow rate, r, is 0.5). This means that in order to achieve the best thermal performance in a double-flow solar air heater, in which the cross-section areas of upper- and lower-flow channels are constructed equally, the mass-flow rates in both flow channels must be the same. The thermal performance decreases when r, as well as $(1-r)$, goes away from 0.5**.** The improvements in collector efficiencies of a double-flow type solar air heaters with fins attached operating at same mass-flow rate in upper- and lower-flow channels, based on a downward-type single-flow device of same size, were calculated by Eq. (20), and the results are presented in Table 1. One may notice in Table 1 that the collector efficiencies of both devices, η^* and η_D, increase with mass-flow rate of air m, while only η_D increases with incident solar radiation S_0. Accordingly, I^* decreases as m or S_0 increase.

It is concluded that providing fins attached on the collector, will improve the collector efficiency. Moreover, constructing the collector with fins attached may scarcely increase the fan power and almost not leading to increased operating cost because the fins employed are usually thin, as compared with the width of collector ($t \ll W$). Consequently, application of the concept of double-flow in the design of a solar air heater with fins attached is technically and economically feasible.

6. Acknowledgment

The authors wish to express our thanks to the National Science Council of the Republic of China for financial aid.

Appendix A

$$B_1 = -h_{r,p-c_1}h_1'G_3G_4 - h_1\phi_1G_3 - U_{c_1-a}h_1'G_4, \tag{A1}$$

$$B_2 = h_1\phi_1G_2 + h_{r,p-c1}h'_1G_2G_4, \tag{A2}$$

$$B_3 = h_1\phi_1G_3 + h_{r,p-c1}h'_1G_3G_4, \tag{A3}$$

$$B_4 = h_2\phi_2G_6 + h_{r,p-R}h'_2G_6G_7, \tag{A4}$$

$$B_5 = -h_{r,p-R}h'_2G_5G_7 - h_2\phi_2G_5 - U_Bh'_2G_7, \tag{A5}$$

$$B_6 = h_2\phi_2G_3 + h_{r,p-R}h'_2G_3G_7, \tag{A6}$$

$$G_1 = (h_2\phi_2 + U_T + U_B)/(U_T + U_B + h_1\phi_1 + h_2\phi_2), \tag{A7}$$

$$G_2 = h_2\phi_2/(U_T + U_B + h_1\phi_1 + h_2\phi_2), \tag{A8}$$

$$G_3 = S_0\alpha_p\tau_g^2/(U_T + U_B + h_1\phi_1 + h_2\phi_2), \tag{A9}$$

$$G_4 = (h_{r,p-c_1} + h'_1 + U_{c_1-a})^{-1}. \tag{A10}$$

$$G_5 = (h_1\phi_1 + U_T + U_B)/(U_T + U_B + h_1\phi_1 + h_2\phi_2), \tag{A11}$$

$$G_6 = h_1\phi_1/(U_T + U_B + h_1\phi_1 + h_2\phi_2), \tag{A12}$$

$$G_7 = (h_{r,p-R} + h'_2 + U_B)^{-1}. \tag{A13}$$

References

[1] Whillier A. Plastic covers for solar collectors. Solar Energy 1963;7:148–54.
[2] Tan HM, Charters WWS. Experimental investigation of forced-convective heat transfer for fully-developed turbulent flow in a rectangular duct with asymmetric heating. Solar Energy 1970;13:121–5.
[3] Close DJ, Dunkle RV. Behaviour of adsorbent energy storage beds. Solar Energy 1976;18:287–92.
[4] Seluck MK. In: Sayigh AAM, editor. Solar air heaters and their applications. New York: Academic Press; 1977.
[5] Kreith F, Kreider JF. Principles of solar engineering. New York: McGraw-Hill, 1978.
[6] Liu CH, Sparrow EM. Convective–radiative interaction a parallel plate channel—application to air-operated solar collectors. Int J Heat Mass Transfer 1980;23:1137–46.
[7] Duffie JA, Beckman WA. In: Solar engineering of thermal processes. 3rd ed. New York: Wiley; 1980.
[8] Yeh HM, Ting YC. Effects of free convection on collector efficiencies of solar air heaters. Appl Energy 1986;22:145–55.
[9] Satcunanathan S, Deonarine SA. Two-pass solar air heater. Solar Energy 1973;15:41–9.
[10] Wijeysundera NE, Ah LL, Tjioe LE. Thermal performance study of two-pass solar air heaters. Solar Energy 1982;28:363–70.
[11] Garg HP, Sharma VK, Bhargava AK. Theory of multiple-pass solar air heaters. Energy 1985;10:589–99.

[12] Yeh HM, Lin TT. The effect of collector aspect ratio on the collector efficiency of flat-plate solar air heaters. Energy 1995;20:1041–7.
[13] Hollick JC, Peter RW. Method and apparatus for heating ventilation air for a building. United States Patent No. 4,934,338; 1990.
[14] Kutscher CF, Christensen C, Barker G. Unglazed transpired solar collectors: an analytic model and test results. Proc ISES Solar World Cong 1991;2:1245–50.
[15] Kutscher CF, Christensen C, Barker G. Unglazed transpired solar collectors: heat loss theory. ASME J Solar Eng 1993;115:182–8.
[16] Kutscher CF. Heat exchanger effectiveness and pressure drop for air flow through perforated plates with and without crosswind. J Heat Transfer 1994;116:391–9.
[17] Gunnewiek LH, Brundrett E, Hollands KGT. Flow distribution in unglazed transpired plate solar air heaters of large area. Solar Energy 1996;58:227–37.
[18] Yeh HM, Ho CD, Hou JZ. The improvement of collector efficiency in solar air heaters by simultaneously air flow over and under the absorbing plate. Energy 1999;24:857–71.
[19] Incropera FP, Dewitt DP. In: Fundamentals of heat and mass transfer. 3rd ed. New York: Wiley; 1990.
[20] Moffat RJ. Describing the uncertainties in experimental results. Exp Thermal Fluid Sci 1988;1:3–17.